Available online at www.sciencedirect.com
SCIENCE DIRECT®
Journal of Chromatography A, 1081 (2005) 156–162
JOURNAL OF CHROMATOGRAPHY A
www.elsevier.com/locate/chroma

Mathematical analysis of affinity membrane chromatography

Wei Shi [a,b,*], Fengbao Zhang [a], Guoliang Zhang [a]

[a] *School of Chemical Engineering & Technology, Tianjin University, Tianjin 300072, China*
[b] *Biomedical Engineering Research Center, Medical College, Xiamen University, Xiamen 361005, China*

Received 6 July 2004; received in revised form 21 February 2005; accepted 19 May 2005
Available online 13 June 2005

Abstract

A mathematical model including convection, diffusion and Freundlich adsorption is developed. To examine the validity of the model, the affinity membranes were prepared by coating chitosan on the nylon membranes, a ligand of poly-L-lysine was bound to the chitoan-coating membranes, and the adsorption behavior of bilirubin through the stacked affinity membranes was investigated. The agreements between the theoretical and experimental results are exceptional. Using our new model, we show that: (1) As *Pe* increases, the breakthrough curves become sharper. For *Pe* greater than 30, the effect of axial diffusion is insignificant; (2) As *m* increases, the time of total saturation is delayed and the loading capacity at the point of breakthrough is increased; (3) As *n* decreases, the time of total saturation is delayed and the loading capacity at the point of breakthrough is increased; (4) As *r* increases, both the time of total saturation and the loading capacity at the point of breakthrough are increased; (5) adsorption rate influences the time of total saturation strongly but contributes little to the loading capacity.

Keywords: Affinity membrane; Freundlich adsorption; Breakthrough curve; Bilirubin

1. Introduction

Affinity chromatography is a powerful biomolecules purification method that is based on the specific interaction between immobilized ligands and target proteins. It is unique among separation methods as it is the only technique that permits the purification of proteins based on biological functions rather than individual physical or chemical properties [1]. The affinity chromatography displays high specificity due to the strong interaction between the ligand and the proteins of interest. However, it suffers from several technical problems including the compressibility, slow mass transfer and adsorption kinetics of the traditional particle media for column chromatography, etc. [2–4].

In an effort to overcome the problems associated with the affinity chromatography, recently, affinity membrane chromatography has attracted much attention because the integration of membrane and affinity chromatography provides a number of advantages over traditional affinity chromatography with porous-bead packed columns, such as higher flow rate, faster binding rate, lower pressure drop, higher productivity and easier scale-up [5,6]. The highly efficient process of affinity membrane chromatography is based on the use of thin layers of finely organized and well-controlled macroporous polymeric stationary phases in the form of rigid disks of 2–3 mm thickness [1,7]. As a result of the convective flow of the solution through the pores, the mass transfer resistance is tremendously reduced. This results in rapid processing, which greatly improves the adsorption, washing, elution, and regeneration steps. Due to the macroporous structure of the membrane support, affinity membrane chromatography has a lower pressure drop, higher flow-rate, and higher productivity than column chromatography. The additional advantages of easy packing and scale-up, as well as the unlikely fouling/clogging, make membrane chromatography an ideal large-scale separation process for the purification and recovery of proteins and enzymes [1,8].

In literatures, very few models have been developed so far to describe the transport phenomenon of affinity membrane chromatography, and the majority is obtained by modifying

* Corresponding author. Tel.: +86 592 2185299.
E-mail address: shiwei@xmu.edu.cn (W. Shi).

0021-9673/$ – see front matter © 2005 Elsevier B.V. All rights reserved.
doi:10.1016/j.chroma.2005.05.031

the models of affinity chromatography. The Thomas model [9] has been used frequently to describe the process of affinity chromatography in a packed column. This model involves Langmuir reaction kinetics as the rate-limiting step. Without mass-transfer effects on column performance, the overall rate of adsorption is only limited by the intrinsic adsorption kinetics. It is suggested that, in membrane column affinity chromatography, the Thomas solution can be used when working with axial Peclet numbers greater than 40 and radial Peclet numbers smaller than 0.04. Suen [10] proposed a model including convection, diffusion and Langmuir adsorption. In this model, the effects of axial diffusion, flow velocity and sorption kinetics on separation performance were discussed. It was found that axial diffusion, which is insignificant in affinity column separation, may dominate over convection at low flow rates or for thin membranes. On the other hand, at high flow velocities, some solutes may pass directly through the membrane without binding due to slow sorption kinetics. Sorption kinetics was shown to dominate affinity membrane performance. The frontal chromatography of lysozyme on an affinity membrane of cellulose–Cibacron Blue was studied by Liu and Fried [11], using the membrane affinity chromatography model, and they explored pore-size distribution and membrane thickness-variation effects on column performance. From their variation analysis, the effects of pore-size distribution and thickness variation for a membrane system are very significant. Frontal chromatography membrane models, which fail to account for extra-column effects, cannot be expected to describe separation performance properly [12,13]. Suen and Etzel [14] extended the membrane affinity chromatography model to study extra-column effects in membrane systems. Their results show that these effects are relevant for a proper description of performance in these type of separations. A theoretical analysis for frontal affinity chromatography in hollow fiber membranes has been also reported [13,15].

The equilibrium adsorption of a solute on an affinity matrix based on the above models is often described simply by the Langmuir equation, with the assumption that single site, homogeneous interaction occurs between the solute and the ligand, and that nonspecific interactions promoted by the support are absent [13,16]. However, practical solids, due to their complex pore and surface structure, rarely conform to the fundamental description, that is very often than not fundamental adsorption isotherm equations such as the classical Langmuir equation do not describe the data well because the basic assumptions made in the Langmuir theory are not readily satisfied.

In this paper, an affinity-membrane model based upon Freundlich equation was developed. The affinity membranes were prepared by coating chitosan on the nylon membranes. A ligand of poly-L-lysine was bound to the chitoan-coating membranes, and the adsorption behavior of bilirubin through the stacked affinity membranes was investigated. The model parameters were obtained by batch experiments, then the utility of the model was demonstrated using experimental data. Finally, system parameters were varied to evaluate their effects on the performances of the system.

2. Theory

2.1. Adsorption kinetics

Langmuir was first to propose a coherent theory of adsorption onto a flat surface based on a kinetic viewpoint, i.e., there is continual process of bombardment of molecules onto the surface and a corresponding desorption of molecules from the surface to maintain zero rate of accumulation at the surface at equilibrium. The assumptions of the Langmuir model are that surface is homogeneous, and adsorption energy is constant over all sites. In fact, because the adsorbent surface is often heterogeneous and/or interaction among adsorbed molecules cannot be neglected, the heat of adsorption varies with the surface coverage. The direct evidence of the solid heterogeneity is the decrease of the isosteric heat of adsorption versus loading. This is because sites of highest energy are usually taken up by adsorbate first and then sites of lower energy are progressively filled [17].

The kinetics equation of Freundlich is

$$r = \frac{\mathrm{d}c_\mathrm{s}}{\mathrm{d}t} = k_{\mathrm{a}0} c \theta_A^{-b_1} - k_{\mathrm{d}0} \theta_A^{b_2} \tag{1}$$

where c and c_s are the solute concentration in the fluid phase and concentration of solute–ligand complex in the solid phase, respectively.

The fractional coverage θ_A can be defined as

$$\theta_A = C_\mathrm{s} = \frac{c_\mathrm{s}}{c_\mathrm{l}} \tag{2}$$

where c_l is the total adsorbed capacity.

At equilibrium, Eq. (1) reduces to the Freundlich model:

$$C_\mathrm{s} = K c^{(1/b)} \tag{3}$$

where, $K = (k_{\mathrm{a}o}/k_{\mathrm{d}o})^{1/b}$ and $b = b_1 + b_2$.

2.2. Model

In the development of a model for the breakthrough curve of a macroporous affinity membrane, the flow of the ligate solution through the membranes is depicted in Fig. 1. It is based on the isothermal sorption of a single ligate during laminar flow through a porous membrane onto which a ligand is immobilized. The feed ligate concentration is c_0. The ligate solution has a concentration $c(z, t)$ with a constant interstitial flow velocity v through a membrane of thickness L, surface area A and void porosity ε. In developing the model, the following assumptions are made: (1) the diffusion coefficient (D), viscosity (μ), and density (ρ) of the ligate solution are constant; (2) mass transport may occur by axial convection and axial diffusion while other transport mechanisms, such as radial diffusion, radial convection or surface diffusion, are

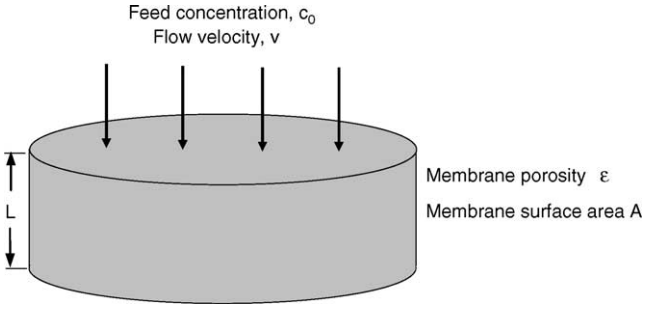

Fig. 1. Stacked flat-sheet affinity membrane model.

negligible; (3) fluid linear velocity is independent of concentration and varies only with radius.

Based upon the assumptions cited above, a mass balance over a section of the membrane gives the following continuity equation [10]:

$$\varepsilon\frac{\partial c}{\partial t}+\varepsilon v\frac{\partial c}{\partial z}=\varepsilon D\frac{\partial^2 c}{\partial z^2}-(1-\varepsilon)\frac{\partial c_s}{\partial t} \tag{4}$$

The basis for affinity separations is the formation of a strong noncovalent bond between the ligand and ligate. The interaction can be described by an equilibrium relationship of the form:

$$\text{Ligand}+\text{ligate}\Leftrightarrow\text{ligand}-\text{ligate}$$

Assume that adsorption between ligand and ligate can be described by kinetics equation of Freundlich, therefore

$$\frac{\partial c_s}{\partial t}=k_{a0}c\left(\frac{c_s}{c_l}\right)^{-b_1}-k_{d0}\left(\frac{c_s}{c_l}\right)^{b_2} \tag{5}$$

The initial conditions are set such that there is no ligate in the membrane.

Initial conditions:

$$c=0\quad\text{at}\quad z\geq 0,\ t=0 \tag{6}$$

$$c_s=0\quad\text{at}\quad z\geq 0,\ t=0 \tag{7}$$

The Danckwerts' boundary conditions [18] are used to account for dispersion at the front surface of the membrane and complete mixing with only convection flow at the exit of the membrane.

Boundary conditions:

$$\varepsilon vc-\varepsilon D\frac{\partial c}{\partial z}=\varepsilon vc_0\quad\text{at}\quad z=0,\ t>0 \tag{8}$$

$$\frac{\partial c}{\partial z}=0\quad\text{at}\quad z=L,\ t>0 \tag{9}$$

In general, axial diffusion should be considered at the entrance of the membrane because a step first-order spatial slope exists there. When axial diffusion is insignificant, i.e. D approaches zero, Eq. (8) reduces to $c=c_0$ at the entrance, which is the case of a step input.

For convenience, we can define the following dimensionless variables:

$$\tau=\frac{vt}{L} \tag{10}$$

$$\zeta=\frac{z}{L} \tag{11}$$

$$C=\frac{c}{c_0} \tag{12}$$

$$C_s=\frac{c_s}{c_l} \tag{13}$$

$$Pe=\frac{vL}{D} \tag{14}$$

$$m=\frac{(1-\varepsilon)c_l}{\varepsilon c_0} \tag{15}$$

$$n=\frac{(1-\varepsilon)k_{a0}L}{\varepsilon v} \tag{16}$$

$$r=1+\frac{c_0}{K_d} \tag{17}$$

Here Pe is the axial Peclet number; m is the ratio of total adsorbed capacity to feed solute concentration; n is the dimensionless number of transfer units; r is the dimensionless separation factor which determines the maximum ligand loaded onto the membrane matrix at equilibrium. K_d is the dissociation equilibrium constant of Freundlich adsorption and is equal to k_{d0}/k_{a0}.

After substitution of the dimensionless groups, Eqs. (4)–(9) become

$$\frac{\partial C}{\partial\tau}+\frac{\partial C}{\partial\zeta}=\frac{1}{Pe}\frac{\partial^2 C}{\partial\zeta^2}-m\frac{\partial C_s}{\partial\tau} \tag{18}$$

$$\frac{\partial C_s}{\partial\tau}=\frac{n}{m}CC_s^{-b_1}-\frac{n}{m(r-1)}C_s^{b_2} \tag{19}$$

Initial conditions:

$$c=0\quad\text{at}\quad\zeta\geq 0,\ \tau=0 \tag{20}$$

$$C_s=0\quad\text{at}\quad\zeta\geq 0,\ \tau=0 \tag{21}$$

Boundary conditions:

$$C-\frac{1}{Pe}\frac{\partial C}{\partial\zeta}=1\quad\text{at}\quad\zeta=0,\ \tau>0 \tag{22}$$

$$\frac{\partial C}{\partial\zeta}=0\quad\text{at}\quad\zeta=1,\ \tau>0 \tag{23}$$

The governing equations are a set of mixed differential equations. Eqs. (18) and (19) are partial differential and nonlinear differential equations, respectively, so they must be solved simultaneously with the initial conditions and boundary conditions. We used the finite-difference method to solve the equations for the model of affinity membrane performance.

3. Experimental

3.1. Chemicals and apparatus

Nylon membranes (47 mm diameter, 0.45 μm pore size) were obtained from Whatman (England). Chitosan (Mr ~40,000) was provided by Fluka (Swizerland). Poly-L-lysine (PLL) and sodium cyanoborohydride were purchased from Sigma (Germany). Bovine serum albumin (BSA) was obtained from Beijing Chemical Reagent Company (China). Bilirubin was purchased from Shanghai Weihui Chemical Factory (China). The other reagents used were bought in China.

A peristaltic pump (Model BT-100, Shanghai, China) was used for the feeding of bilirubin solutions. The concentration of bilirubin and albumin-conjugated bilirubin were determined using a 752N UV–vis spectrophotometer (Shanghai Precision Instruments Co. Ltd., Shanghai, China). The membrane cartridge (donated amicably from the Dalian Chemical and Physical Institute, China) was used to load the membrane stack.

3.2. Affinity-membrane preparation

3.2.1. Preparation of chitosan-coated membrane

Nylon membrane disks (47 mm diameter) were shaken in 1 M HCl for 24 h at room temperature. After partial hydrolysis of amide bonds, the membranes were shaken in 20% (v/v) epibromohydrin solution, pH 11, adjusted by NaOH, at 60 °C for 10 h. After activation, the membranes were washed three times for 20 min with water at room temperature [19].

The activated membranes were shaken in 10 mL chitosan solution (prepared by dissolving 0.15 g chitosan in 10 mL 1 vol.% acetic acid solution) for 30 min at room temperature. The chitosan solution was then sucked through the membranes, which were subsequently incubated in an oven at 80 °C for 10 h. Non-covalently bound chitosan was removed by washing the membranes with 1 vol.% acetic acid solution and deionized water.

3.2.2. Immobilization of PLL

An amount of 80 mg of sodium borohydride was dissolved in 12 mL 2 M NaOH. Then 20 mL of water and 4 mL of epibromohydrin were added. One chitosan-coated membrane was shaken in epibromohydrin solution for 3 h at 50 °C. Finally, the membrane was washed at least three times with deionized water [19,20].

After activation, chitosan-coated membranes were incubated in 0.2 M sodium periodate for 90 min at room temperature. An amount of 60 mg sodium cyanoborohydride and 100 mg of PLL hydrobromide were dissolved in 10 mL 0.1 M phosphate buffer and adjusted to pH 7.0. One periodate-activated chitosan-coated membrane was given in PLL solution and shaken overnight at room temperature. Afterwards the membranes were washed with 1 M NaCl and deionized water extensively.

3.3. Dynamic adsorption of bilirubin

The dynamic experiments were carried out in the cartridge to investigate the breakthrough performance. Bilirubin-phosphate buffer solution (200 mg/L) was impelled by peristaltic pump with two different flow rate (i.e. 4 and 6 mL/min) to flow through the membrane stack (containing five overlapped membranes) in a single-pass mode. Then the amounts of bilirubin through the membrane cartridge were measured in succession with a spectrophotometer [19,21].

4. Determination of model parameters

4.1. The parameters ε and D

The porosity ε was measured by determining the amount of water adsorbed by the membranes [22] and the axial diffusion coefficient D was determined from experimental measurements [23,24].

4.2. The parameter c_l

PLL-attached membranes were equilibrated by shaking in saturated bilirubin-phosphate buffer solution. The amount of bilirubin adsorbed on membranes (m_b) was measured by spectrophotometry at the wavelength of 438 nm. Then, c_l can be calculated by

$$c_l = \frac{m_b}{AL(1-\varepsilon)M_b} \tag{24}$$

where M_b is the molecular weight of bilirubin.

4.3. The parameters K_d and b

We have applied Freundlich adsorption isotherms for the description of the adsorption mechansim for bilirubin on PLL-attached membrane [19]. Fig. 2 shows the linear relationship of the Freundlich isotherm for the adsorption of bilirubin with PLL-attached membranes, where q is adsorption capacity (mg) of bilirubin; X is the weight of the membrane in grams; c is the bilirubin concentration. From this figure and the value of c_l, we can obtained the values of K and b. Thus the value of K_d can be easily calculated from its definition.

4.4. The parameters b_2 and k_{d0}

After adsorption of bilirubin onto the PLL-attached membranes, the membranes which have been known the amount of adsorbed bilirubin were shaken in BSA solution at 37 °C. Concentration of BSA-conjugated bilirubin was measured by spectrophotometry at the wavelength of 460 nm at a given interval. BSA (Albumin) is known to be natural carriers of

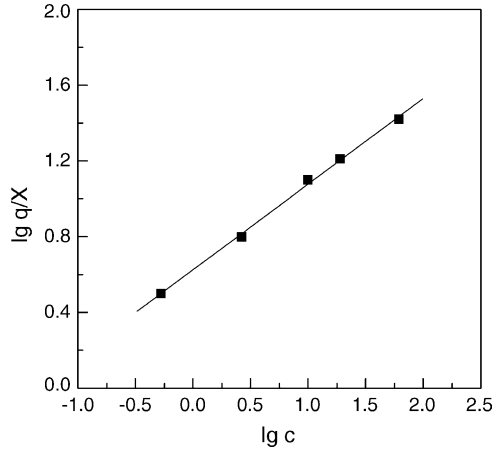

Fig. 2. Freundlich adsorption isotherm of PLL for bilirubin at 37 °C.

bilirubin. It is generally agreed that each albumin molecule can bind two bilirubin molecules strongly [21,25], so the bilirubin molecules desorbed from the membranes will be bound albumin molecule immediately. Therefore, the Eq. (5) can be written as

$$\frac{dc_s}{dt} = -k_{d0}\left(\frac{c_s}{c_l}\right)^{b_2} \tag{25}$$

By carrying out integration, one obtains

$$c_s^{1-b_2} = c_{s,0}^{1-b_2} - \frac{k_{d0}(1-b_2)}{c_l^{b_2}}t \tag{26}$$

Because

$$\delta c_{s,i} = \frac{c_{s,i+1} - c_{s,i-1}}{2\Delta t} \approx \frac{dc_{s,i}}{dt} = -k_{d0}\left(\frac{c_s}{c_l}\right)^{b_2} \tag{27}$$

Then

$$\log(-\delta c_{s,i}) = b_2 \log c_{s,i} + (\log k_{d0} - b_2 \log c_l) \tag{28}$$

As shown in Fig. 3, a straight line is obtained by plotting $\log(-\delta c_{s,i})$ as a function of $\log c_{s,i}$. From slope and intercept of the line, the values of b_2 and k_{d0} are obtained. Furthermore the values of b_1 and k_{ao} can be calculated through the equations of $K = (k_{a0}/k_{d0})^{1/b}$ and $b = b_1 + b_2$.

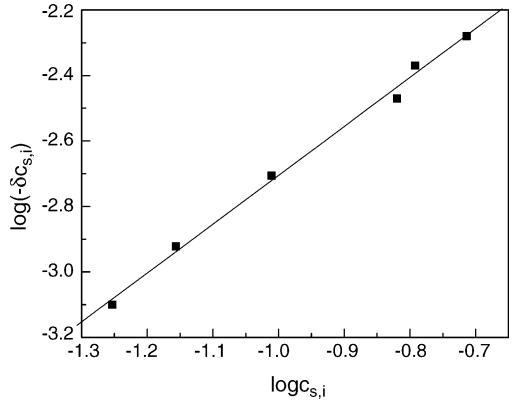

Fig. 3. Curve of $\log(-\delta c_{s,i}) - \log c_{s,i}$.

Table 1
The parameter values for the model

ε	c_1 (mol/L)	K_d (mol/L)	D (m^2/s)
0.62	0.026	8.2×10^{-5}	1.18×10^{-9}
b_1	b_2	k_{ao} (1/s)	k_{d0} (mol/L s)
0.57	1.49	1.58	1.29×10^{-4}

The values of parameters obtained are shown in Table 1.

5. Results and discussion

Most affinity separations are operated in the frontal analysis mode. This includes continuous flow of the ligate solution into the inlet until a breakthrough occurs as indicated by detection of the ligate at the system outlet. The plot of effluent concentration of the ligate versus time or throughput volume is called the breakthrough curve. In this model analysis, dimensionless breakthrough curves where dimensionless effluent concentration is plotted versus dimensionless time were used. Breakthrough and saturation are defined as that points where the exit ligate concentration in the fluid phase equals 10 and 99% of the inlet concentration, respectively. The loading capacity is defined as the amount of ligate bound to the membrane at the point of breakthrough.

5.1. The effects of model parameters on breakthrough curve

The effect of axial diffusion is represented by the axial Pelect number, *Pe*. The breakthrough curves for different *Pe* are illustrated in Fig. 4. At low *Pe*, the axial diffusional flux is very high so that concentration of ligate is dispersed along the axial direction. Under this condition, the breakthrough curves are broadened, the time of total saturation is delayed and the loading capacity at the point of breakthrough is decreased. As *Pe* increases, the breakthrough curves become sharper. For *Pe* greater than 30, the effect of axial diffusion is insignificant.

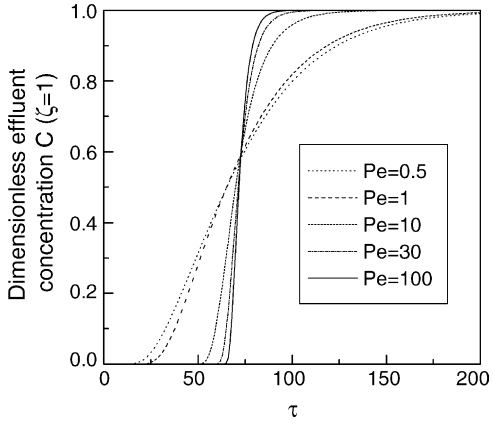

Fig. 4. The effect of axial diffusion on the shape of the breakthrough curve ($m = 38.57$; $n = 23.36$; $r = 5.52$; $b_1 = 0.8$; $b_2 = 1.5$).

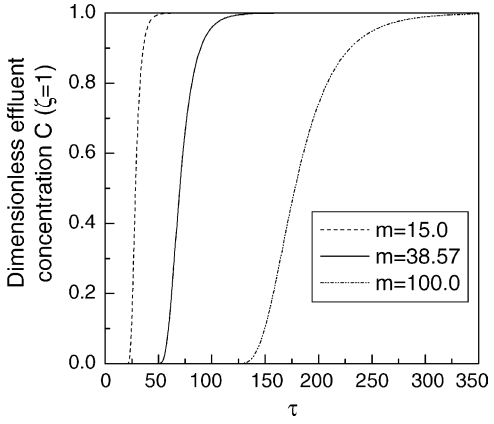

Fig. 5. The effect of ratio of total ligand capacity to feed concentration on the breakthrough curve ($Pe = 10$; $n = 23.36$; $r = 5.52$; $b_1 = 0.8$; $b_2 = 1.5$).

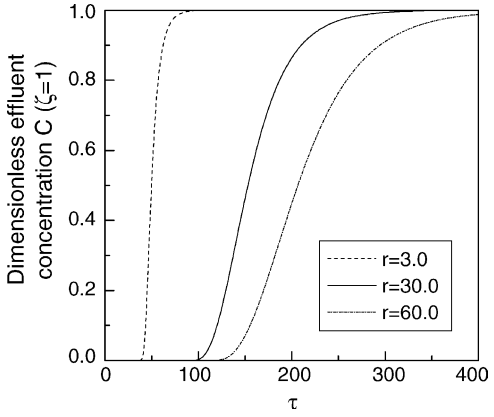

Fig. 7. The effect of the separation factor on the breakthrough curve ($Pe = 10$; $m = 38.57$; $n = 23.36$; $b_1 = 0.8$; $b_2 = 1.5$).

Axial diffusion should be important only for thin membranes. As the membrane thickness increases, *Pe* also increases, and the effect of axial diffusion decreases to a negligible level. If the membrane thickness is increased in a given affinity membrane system, *Pe* increases with the square of the membrane thickness. The relationship can be derived with all other parameters held constant by substituting Eq. (16) into Eq. (14). This is in accordance with the model of Suen [10].

The model parameter *m* is the ratio of maximum capacity of ligate adsorbed on the ligand to feed solute concentration. A large *m* corresponds to a small feed concentration or a large capacity of ligate adsorbed. When all other parameters are set constant, the parameter *m* mainly shows the effect of ligand capacity on the breakthrough curves. The breakthrough curves for different *m* are shown in Fig. 5. As *m* increases, the time of total saturation is delayed and the loading capacity at the point of breakthrough is increased.

The dimensionless number of transfer units *n* is proportional to k_{a0}. The effect of *n* on the breakthrough curves is shown in Fig. 6. As *n* decreases, the time of total saturation is delayed and the loading capacity at the point of breakthrough is increased. When $n = 1$, the breakthrough curve has been metamorphosed severely. We argue that this results from the small adsorption velocity of the ligate on ligand, so the membrane is easily penetrated through.

The dimensionless separation factor, *r*, which determines the maximum ligand loaded onto the membrane matrix at equilibrium is proportional to feed solute concentration, and inversely proportional to the dissociation equilibrium constant of Freundlich adsorption. The breakthrough curves for different *r* are illustrated in Fig. 7. As *r* increases, both the time of total saturation and the loading capacity at the point of breakthrough are increased. This is because of adsorption capacity is proportional to *r*.

The effects of b_1 and b_2 on the breakthrough curves are shown in Figs. 8 and 9, respectively. As b_1 and b_2 decrease, the time of total saturation is delayed. But the loading capacity at the point of breakthrough is nearly independent of b_1 and b_2. From Eq. (5), we know that adsorption rate decreases as b_1 and b_2 ($b = b_1 + b_2$) decrease. Therefore, it is reasonable to conclude that adsorption rate influences the time of total saturation strongly but contributes little to the loading capacity.

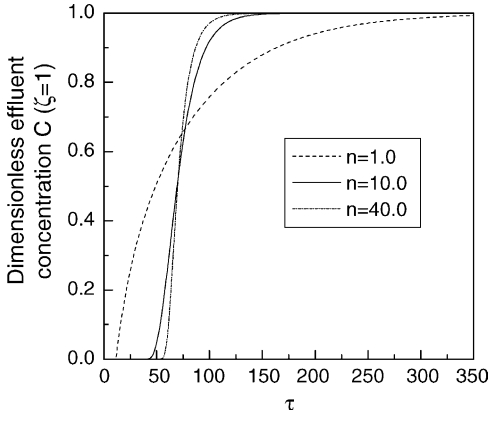

Fig. 6. The effect of the number of transfer units on the breakthrough curve ($Pe = 10$; $m = 38.57$; $r = 5.52$; $b_1 = 0.8$; $b_2 = 1.5$).

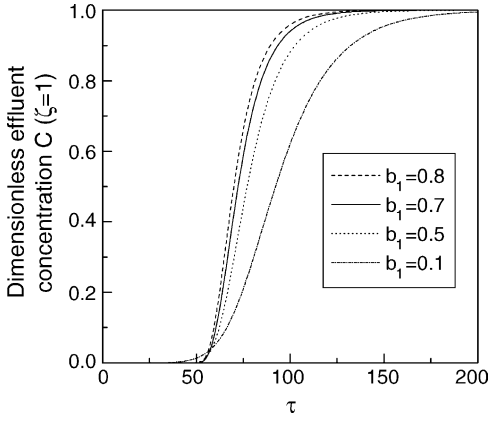

Fig. 8. The effect of b_1 on the shape of the breakthrough curve ($Pe = 10$; $m = 38.57$; $n = 23.36$; $r = 5.52$; $b_2 = 1.5$).

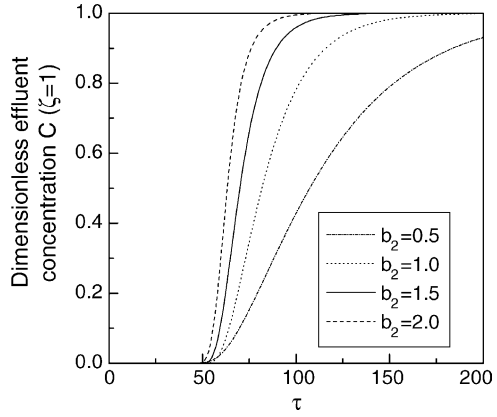

Fig. 9. The effect of b_2 on the shape of the breakthrough curve ($Pe = 10$; $m = 38.57$; $n = 23.36$; $r = 5.52$; $b_1 = 0.8$).

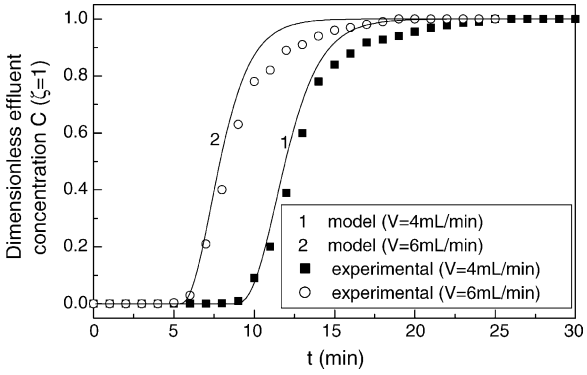

Fig. 10. The comparison between the model prediction and experimental data.

5.2. Model simulation

The values of parameters have been given in Table 1. The comparison between the theoretical predictions and the experimental results is shown in Fig. 10 for bilirubin adsorption by the PLL-attached affinity membrane. It can be seen that the prediction is consistent with the experimental data. From Fig. 10 we can see that: when $\zeta < 0.6$, the model predictions are in good agreement with the experimental data, and when $\zeta > 0.6$, the relative error between the theoretical and experimental data increases. The practical breakthrough curves are gently broader than theoretical, and the time of total saturation of practical breakthroughs is delayed compared with the model predictions. The deviation of the breakthrough curves between the model predictions and experimental data may be due to the following reasons. The membranes may have some dead volume which cannot be reached by convective flow. When membranes are stacked, more dead volume may also be created. The adsorption of the ligand in the dead volume would be limited by the slow diffusion of the ligate through the dead space.

Acknowledgement

We are in deep debt to the National Nature Science Foundation of China for supporting this research (No.29776036).

References

[1] H.F. Zou, Q.Z. Luo, D.M. Zhou, J. Biochem. Biophys. Meth. 49 (2001) 199.
[2] L. Yang, W.W. Hsiao, P. Chen, J. Membrane Sci. 197 (2002) 185.
[3] M. Unaska, P.A. Davies, M.P. Esnouf, B.J. Bellhouse, J. Chromatogr. 519 (1990) 53.
[4] M. Nachman, A.R.M. Azad, J. Bailon, J. Chromatogr. 597 (1992) 155.
[5] M. Nachman, J. Chromatogr. 597 (1992) 167.
[6] H.Y. Gan, Z.H. Shang, J.D. Wang, J. Chromatog. A 867 (2000) 161.
[7] T.B. Tennikova, M. Bleha, F. Svec, T.V. Almazova, B.G. Belenkii, J. Chromatogr. 555 (1991) 97.
[8] F. Dosio, S. Arpicco, S. Canevari, M. Figini, D. Gastaldi, J. Chromatogr. A 830 (1999) 329.
[9] H.C. Thomas, J. Am. Chem. Soc. 66 (1944) 1664.
[10] S. Suen, Chem. Eng. Sci. 47 (1992) 1355.
[11] H. Liu, J.R. Fried, AIChE J. 40 (1994) 40.
[12] D.K. Roper, E.N. Lightfoot, J. Chromatogr. A 702 (1995) 3.
[13] A. Tejeda-Mansir, R.M. Montesinos, R. Guzman, J. Biochem. Biophys. Meth. 49 (2001) 1.
[14] S. Suen, M.R. Etzel, J. Chromatogr. A 686 (1994) 179.
[15] G.C. Serafica, J. Pimbley, G. Belafort, Biotechnol. Bioeng. 43 (1993) 21.
[16] A.I. Liapis, M.A. McCoy, J. Chromatogr. A 660 (1994) 85.
[17] D.D. Duong, Adsorption Analysis: Equilibria and Kinetics, Imperial College Press, London, 1998.
[18] P.V. Danckwerts, Chem. Eng. Sci. 2 (1953) 219.
[19] W. Shi, F.B. Zhang, G.L. Zhang, L.Q. Jiang, Y.J. Zhao, S.L. Wang, Mol. Simulat. 29 (2003) 787.
[20] D. Petsch, T.C. Beeskow, F.B. Anspach, W.B. Deckwer, J. Chromatogr. B 693 (1997) 79.
[21] W. Shi, F.B. Zhang, G.L. Zhang, L.Q. Jiang, S.L. Wang, H. Xu, Mol. Simulat. 30 (2004) 117.
[22] W. Shi, F.B. Zhang, G.L. Zhang, D.T. Ge, Q.Q. Zhang, Polym. Int. 54 (2005) 790.
[23] D.L. Koch, J.F. Brady, J. Fluid Mech. 154 (1985) 399.
[24] F.H. Arnold, H.W. Blanch, C.R. Wilke, Chem. Eng. J. 30 (1985) 25.
[25] X.X. Zhu, G.R. Brown, L.E. St-Pierre, Biomat. Art. Cells Art. Org. 18 (1990) 75.